

# Incoherent collisions between two-dimensional bright steady-state photorefractive spatial screening solitons

Ming-feng Shih and Mordechai Segev

*Department of Electrical Engineering and Center for Photonics and Optoelectronic Materials,  
Princeton University, Princeton, New Jersey 08544*

Received April 29, 1996

We report the observation of incoherent collisions between two-dimensional bright photorefractive screening solitons. The solitons remain intact and do not exchange energy whenever the collision angle exceeds the critical angle for guidance in the waveguide that each soliton induces, which is, in turn, fully controlled by the soliton parameters. When the collision angle is much smaller than the critical angle the solitons fuse to form a single beam. © 1996 Optical Society of America

Photorefractive spatial solitons<sup>1-10</sup> have attracted much interest recently because they exist at very low powers (microwatts) and in two transverse dimensions. At present, three generic types of photorefractive soliton are known: quasi-steady-state,<sup>1,2,9</sup> photovoltaic,<sup>3</sup> and screening<sup>4-8</sup> solitons. All these solitons form when diffraction is balanced by photorefractive self-focusing effects, and they also induce a planar (or circular) waveguide<sup>3,8-10</sup> that can guide a second, possibly more intense, beam at a less photosensitive wavelength. In a previous Letter<sup>10</sup> we demonstrated circular waveguides induced by two-dimensional bright screening solitons and showed that the number of guided modes depends on the ratio between the peak intensity of the soliton and the sum of the background illumination ( $I_b$ ) and the equivalent dark irradiance ( $I_d$ ) (the so-called intensity ratio). Applications such as reconfigurable near-field multichannel-to-multichannel optical interconnects thus become feasible. It is now necessary to deal with the problem of collision between solitons when one soliton intersects another in the volume of a photorefractive crystal.

Collision of spatial solitons in a photorefractive material is an intriguing issue. Intuitively, one may view soliton collisions in terms of waveguide theory, with the exception that these waveguides are self-induced.<sup>11</sup> Thus collisions of solitons can be described as coupling between the waveguides that they induce and are subject to their guiding properties, e.g., being single mode or multimode, critical angle for guidance, and numerical aperture.<sup>12</sup> For photorefractive soliton collisions one expects an additional interaction between the solitons: two-wave mixing. When two mutually coherent plane waves cross each other in a photorefractive material, the interference grating between them gives rise to a refractive-index grating that causes energy to transfer from one to the other. Since this interaction is between beams rather than between plane waves, it is more complicated than the traditional two-wave mixing model that applies to a low-visibility interference grating. We choose first to analyze collisions between solitons that do not form a stationary interference grating and thus do not exhibit the photorefractive energy-exchange interaction. We therefore study

incoherent collisions between solitons and use two soliton beams that are incoherent with each other, leaving the coherent collisions for a future study. In the present study the relative phase between the soliton beams varies much faster than the response time of the photorefractive medium (dielectric relaxation time), and the collision is unaffected by it.

In this Letter we report the observation of incoherent collisions between two-dimensional bright photorefractive screening solitons. The solitons remain intact and do not exchange energy whenever the collision angle exceeds the critical angle for guidance in the effective waveguide that each soliton induces, which is, in turn, fully controlled by the soliton parameters. When the collision angle is much smaller than the critical angle, the solitons fuse to form a single beam. Similar ideas were suggested for spatial solitons in non-Kerr nonlinear media by use of the self-induced waveguide approach<sup>12</sup> and for temporal solitons in saturable nonlinear media.<sup>13</sup> Recently, collision and fusion of spiraling two-dimensional bright solitons in a saturable nonlinear medium were observed.<sup>14</sup>

Photorefractive screening solitons are characterized by an existence curve of the soliton width  $\Delta\xi$  as a function of intensity ratio.<sup>5,6</sup> Here  $\Delta\xi = \Delta x k n_b^2 (r_{\text{eff}} V / l)^{1/2}$ , with  $\Delta x$  the FWHM of the soliton intensity ( $I$ ) profile,  $k$  the wave number in vacuum,  $n_b$  the refractive index,  $r_{\text{eff}}$  the electro-optic coefficient, and  $V$  the voltage applied across the crystal of width  $l$ . This relation was derived for one-dimensional bright and dark solitons and was verified experimentally.<sup>8,15</sup> It implies that a one-dimensional screening soliton of a specific diameter and at a given intensity ratio can be generated at a single value of applied field. For two-dimensional bright screening solitons we found experimentally<sup>7</sup> a similar trend: A circular soliton of a given diameter and at a specific intensity ratio exists at a single value of applied field. When the field deviates within 5–20% of the correct value the soliton becomes elliptical.<sup>7</sup> Deviations smaller than  $\approx 5\%$  are restrained by the (stable) soliton, and those larger than 20% lead to beam breakup (field too high) or diverging beams (field too low). The intensity ratio also determines the guiding properties

of the waveguide induced by the screening soliton. We have found<sup>10</sup> that at an intensity ratio of  $\leq 25$  the induced waveguide is single mode and that the number of guided modes increases with increasing intensity ratio. Accordingly, the critical angle for guiding in the soliton-induced waveguide increases with increasing intensity ratio because solitons of the same size at higher intensity ratios induce wider and deeper waveguides. In all cases the soliton is the fundamental guided mode of the waveguide that it induces.

One can understand incoherent collisions between solitons by comparing the collision angle with the critical guiding angle in each soliton-induced waveguide. When the collision angle is larger than the critical angle the beam emerging from one soliton-induced waveguide cannot excite a guided mode in the other induced waveguide; instead it refracts twice and passes through the other waveguide, remaining restricted to its own waveguide. In this event the colliding solitons are unaffected by the collision. When the collision angle is shallower than the critical angle, the waveguides become coupled, and energy is transferred from one soliton to another. When the solitons induce multimode waveguides, the energy transferred in the collision process will also excite high-order modes in the plane of the collision, thus breaking the circular symmetry of both colliding solitons. Furthermore, energy can be transferred from the fundamental mode (soliton) in each waveguide to higher guided modes within the same waveguide. Because the soliton is the fundamental guided mode of its own induced waveguide, the additional energy in the higher modes changes the intensity distribution of the soliton.<sup>16</sup> We thus expect that the soliton will deviate from its circular shape in a manner that depends on how much energy is transferred to higher-order modes.

The experimental setup is similar to that of Ref. 7, with two soliton beams, labeled A and B. The optical path difference between the input beams A and B is 0.9 m, much longer than the coherence length of the 488-nm argon-ion laser when its étalon is removed. Both beams A and B are extraordinarily polarized; each has 2  $\mu$ W of power and is circular, with an 11- $\mu$ m diameter at the crystal input face. The crystal is strontium barium niobate with  $r_{\text{eff}} = 180 \times 10^{-12}$  m/V and  $n = 2.35$ , in which beam A propagates parallel to its crystalline  $a$  axis and beam B deviates by a small angle from it toward the  $c$  axis. The angle  $\theta$  is small enough inside the crystal ( $< 6^\circ$ ) that the effective electro-optic coefficient  $r_{33} \cos^3 \theta$  for beam B is close to that of beam A ( $r_{33}$ ). We make sure that these two beams indeed intersect (collide) in the crystal, and, as in Ref. 7, we also illuminate the whole crystal with an additional, uniform, ordinarily polarized beam to generate the background illumination.

First, we generate solitons A and B with intensity ratio 20 by applying an external voltage of 2.1 kV between electrodes separated by 5.5 mm and adjust the collision angle to  $1.2^\circ$  (all angles are measured inside the crystal). As shown below, at this voltage the critical guiding angle is  $\approx 0.5^\circ$ . Figure 1(A) shows the profiles of beams A and B at the input face of the crystal. With no voltage applied, both beams diffract

to  $\sim 50 \mu\text{m}$  in the crystal and overlap at the output face [Fig. 1(B)]. By blocking beam A or B we adjust the voltage and generate individual solitons [Fig. 1(C)]. We then launch both solitons and observe their collision. As shown in Figs. 1(D) and 2(C), the solitons are not affected by the collision, and the energy transferred from one another is less than 2%. Because at this intensity ratio the soliton-induced waveguide is single mode and the higher-order guided modes do not exist, the solitons are not affected by the collision. We then repeat this procedure under the same applied-voltage and intensity-ratio conditions with the collision angle adjusted to  $2.5^\circ$  and to  $0.6^\circ$ . At a collision angle of  $2.5^\circ$  [Fig. 2(E)] the result resembles that of  $1.2^\circ$ , with less than 1% of the energy exchanged between the solitons. At a collision angle of  $0.6^\circ$ , which is roughly the critical guiding angle, we observe that the energy transferred from A to B and vice versa is 10%. However, the solitons are not distorted [Fig. 2(A)] because higher-order modes do not exist at this intensity ratio and thus cannot be excited by the collision. Top-view photographs of the colliding solitons for these three collision angles are shown in Figs. 3(A)–3(C). Figure 3(D) shows, for comparison, the intersecting beams (no solitons) at zero voltage. The diffraction of beams A and B makes these beams almost indistinguishable at the output face of the crystal.

We then increase the intensity ratio to  $\sim 100$ , at which the soliton-induced waveguides are multimode and the critical guiding angle is somewhat smaller than  $1.3^\circ$ . With collision angle  $1.2^\circ$  or  $2.5^\circ$ , solitons A and B pass through each other [Figs. 2(D) and 2(F)], with energy exchange less than 2% and 1%, respectively. Because higher-order modes now exist and can be excited by the collision, both soliton beams are distorted and become elliptical. When we reduce the collision angle to  $0.6^\circ$  the two colliding solitons start to merge [Fig. 2(B)] because the collision angle is well below the critical guiding angle. When we adjust the collision angle to be  $0.2^\circ$  at intensity ratio 120

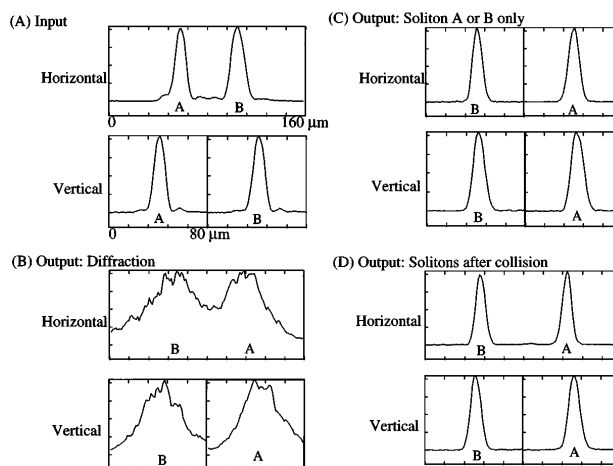


Fig. 1. Horizontal and vertical profiles of beams A and B, both of intensity ratio 20 and crossing angle  $1.2^\circ$ , (A) at the entrance face of the crystal and at the exit face when (B) both beams diffract (zero voltage), (C) soliton A or B forms when the other is blocked, and (D) A and B collide.

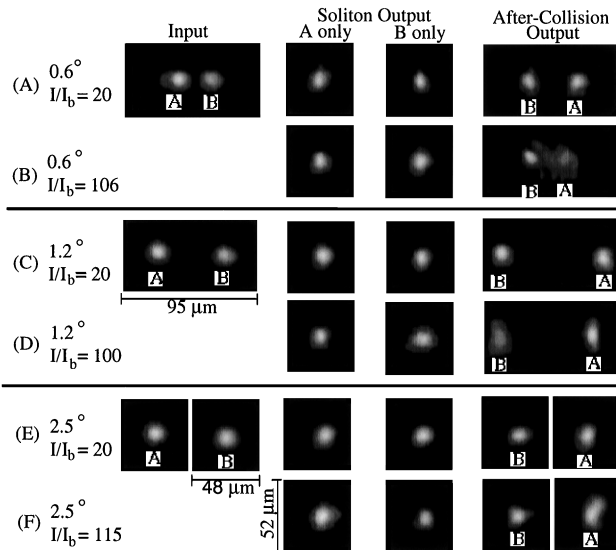


Fig. 2. Photographs of beams A and B at the entrance face (leftmost column) and at the exit face: middle two columns for each soliton when the other is blocked and rightmost columns when both beams are presented, with different collision angles and intensity ratios.

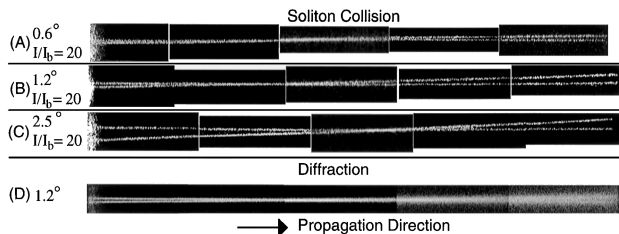


Fig. 3. Top-view photographs of soliton collisions at different colliding angles: (A)–(C) with intensity ratio 20 and (D) when both beams diffract.

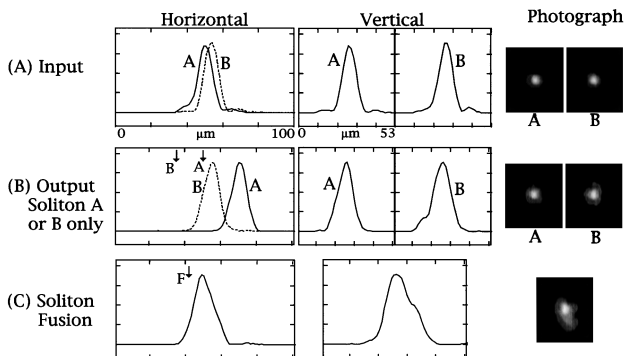


Fig. 4. Profiles and photographs of (A) beams A and B at the entrance face, (B) each soliton at the exit face when the other is blocked, and (C) the fused beam at the exit face. Arrows A and B indicate the positions of the centers of diffracting beams A and B. Arrow F indicates the middle point of arrows A and B.

the solitons fuse to form a single beam at the crystal output face.

Screening solitons also self-bend<sup>7,17</sup> toward the *c* axis as a result of a diffusion space-charge field proportional to  $I'/(I + I_b + I_d)$ , where  $I$  is the intensity profile and  $I'$  is the derivative of  $I$  with respect to the transverse direction. This self-bending is affected by the collisions when the solitons distort or fuse, the lat-

ter being rather a significant effect. The fused beam is wider than each soliton, thus reducing the self-bending. One can see this from Figs. 4(B) and 4(C) by comparing the average bending of the individual A and B solitons (arrow F) with the center of the fused beam.

In conclusion, we have reported the observation of incoherent collisions between two-dimensional bright photorefractive screening solitons and found a behavior similar to that predicted for solitons in saturable nonlinear media.<sup>12,13</sup> Future research will be directed toward evaluating and measuring the reflection–transmission constants of a system with colliding solitons, as suggested for Kerr solitons.<sup>18</sup>

M. Segev gratefully acknowledges the support of a Sloan Fellowship. This research was supported by the U.S. Army Research Office.

## References

1. M. Segev, B. Crosignani, A. Yariv, and B. Fischer, *Phys. Rev. Lett.* **68**, 923 (1992).
2. G. Duree, J. L. Shultz, G. Salamo, M. Segev, A. Yariv, B. Crosignani, P. DiPorto, E. Sharp, and R. Neurgaonkar, *Phys. Rev. Lett.* **71**, 533 (1993).
3. G. C. Valley, M. Segev, B. Crosignani, A. Yariv, M. M. Fejer, and M. Bashaw, *Phys. Rev. A* **50**, R4457 (1994); M. Taya, M. Bashaw, M. M. Fejer, M. Segev, and G. C. Valley, *Phys. Rev. A* **52**, 3095 (1995).
4. The steady-state self-focusing effect was first observed by M. D. Iturbe-Castillo, P. A. Marquez-Aguilar, J. J. Sanchez-Mondragon, S. Stepanov, and V. Vysloukh, *Appl. Phys. Lett.* **64**, 408 (1994).
5. M. Segev, G. C. Valley, B. Crosignani, P. DiPorto, and A. Yariv, *Phys. Rev. Lett.* **73**, 3211 (1994); M. Segev, M. Shih, and G. C. Valley, *J. Opt. Soc. Am. B* **13**, 706 (1996).
6. D. N. Christodoulides and M. I. Carvalho, *J. Opt. Soc. Am. B* **12**, 1628 (1995).
7. M. Shih, M. Segev, G. C. Valley, G. Salamo, B. Crosignani, and P. DiPorto, *Electron. Lett.* **31**, 826 (1995); *Opt. Lett.* **21**, 324 (1996).
8. Z. Chen, M. Mitchell, M. Shih, M. Segev, M. Garrett, and G. C. Valley, *Opt. Lett.* **21**, 629 (1996).
9. M. Morin, G. Duree, G. Salamo, and M. Segev, *Opt. Lett.* **20**, 2066 (1995).
10. M. Shih, M. Segev, and G. Salamo, *Opt. Lett.* **21**, 931 (1996).
11. A. W. Snyder, D. J. Mitchell, and Y. S. Kivshar, *Mod. Phys. Lett. B* **9**, 1479 (1995).
12. This insight was pioneered by A. W. Snyder and A. P. Sheppard, *Opt. Lett.* **18**, 482 (1993), for general non-Kerr nonlinear media.
13. S. Gatz and J. Herrmann, *IEEE J. Quantum Electron.* **28**, 1732 (1992).
14. V. Tikhonenko, J. Christou, and B. Luther-Davies, *Phys. Rev. Lett.* **76**, 2698 (1996).
15. K. Kos, H. Meng, G. Salamo, M. Shih, M. Segev, and G. C. Valley, *Phys. Rev. E* **53**, R4330 (1996).
16. This effect differs from those of previous experiments with soliton-induced waveguides,<sup>10</sup> in which the material was not affected by the guided beam of a much less photosensitive wavelength.
17. S. R. Singh and D. N. Christodoulides, *Opt. Commun.* **118**, 569 (1995).
18. P. D. Miller and N. N. Akhmediev, *Phys. Rev. E* **53**, 4098 (1996).